第2回地震時保有耐力法に基づく橋梁の耐震設計
に関するシンポジウム講演論文集 (1998年12月)

Two Hysteretic Models and Seismic Analysis of Pipe-section Steel Bridge Piers

Qingyun Liu[1], Akira Kasai[2], and Tsutomu Usami[3]

[1] Student Member of JSCE, M. of Eng., Graduate Student, Dept. of Civil Eng., Nagoya University
[2] Member of JSCE, M. of Eng., Research Associate, Dept. of Civil Eng., Nagoya University
[3] Fellow of JSCE, Dr. of Eng., Dr. of Sc., Professor, Dept. of Civil Eng., Nagoya University

1. Introduction

Inelastic seismic response analysis of single bridge piers modeled as SDOF systems requires quick and reliable prediction of hysteretic behavior of the structure. 2-parameter model[1)] based on cyclic tests of box-section steel columns is a typical phenomenological model that simulates hysteretic behaviors through a set of hysteretic rules and a few empirical parameters. Damage evaluation of box-section steel bridge piers shed new light on strength and stiffness degradation of thin-walled steel bridge piers under seismic conditions, and prompted the development of the damage-based hysteretic model[2)]. Since hysteretic behavior of the pipe-section steel bridge piers is quite similar to that of box-section piers, both models can well be extended for use with pipe-section steel bridge piers providing that the model parameters be properly adapted. This study presents model parameters of 2-parameter model (2-para model) and the damage-based hysteretic model (D model)[3)] for pipe-section steel bridge piers, and compares the predicted seismic responses under these two conceptually different hysteretic models.

The original 2-parameter model actually consisted of three sub-models with different hysteretic rules, named type A, B and C. Each type applies to a group of bridge piers whose structural parameters fall within a specified range, and the three combined to cover the entire range of structural parameters of practical interest. In adapting 2-parameter model for use with pipe-section steel bridge piers, it is recognized that by varying model parameters continuously with structural parameters, an integrated model may as well cover the whole possible range of structural parameters without type classification. In what follows, only the integrated 2-parameter model for pipe-section steel bridge piers is presented.

2. Integrated 2-parameter model

(1) Skeleton curve

Fig.1 shows the trilinear skeleton curve of 2-para model. It takes five quantities to fully determine this curve: H_y, δ_y, H_m, δ_m and K_d. Given a certain steel bridge pier, H_y and δ_y are the yield load and yield displacement respectively, which can be calculated analytically; (H_m, δ_m) defines the peak loading point that can be reached under cyclic loading. For pipe-section steel bridge piers, δ_m and H_m have been summarized from cyclic FEM analysis results[4)]:

$$\frac{H_m}{H_y} = \frac{0.02}{(R_t\bar{\lambda})^{0.8}} + 1.10 \tag{1}$$

$$\frac{\delta_m}{\delta_y} = \frac{1}{3(R_t\bar{\lambda}^{-0.5})^{0.8}} - \frac{2}{3} \tag{2}$$

wherein R_t = radius thickness ratio parameter; $\bar{\lambda}$ = slenderness ratio parameter. R_t and $\bar{\lambda}$ for pipe-section steel bridge piers are defined as:

$$R_t = \sqrt{3(1-\nu^2)}\frac{\sigma_y}{E}\frac{D}{2t} \tag{3}$$

$$\bar{\lambda} = \frac{2h}{r}\frac{1}{\pi}\sqrt{\frac{\sigma_y}{E}} \tag{4}$$

wherein σ_y is yield stress of steel; E is Young's modulus; ν is Poisson's ratio; D and t are diameter and thickness of the cross section respectively; h is column height and r radius of gyration of the cross section.

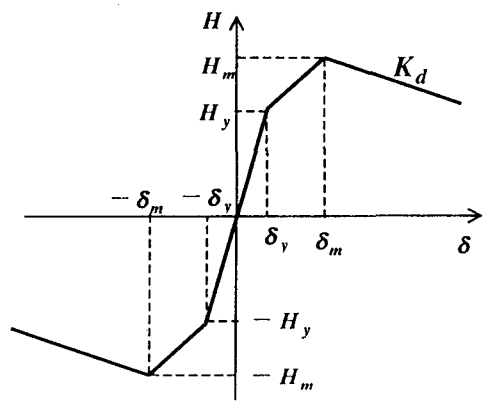

Fig.1 Skeleton curve (2-para model)

Stiffness of the descending branch, K_d, is supposed to be equal to that of monotonic horizontal load—displacement curve, and based on monotonic FEM analysis results, it is approximated by:

$$K_d \frac{\delta_{y0}}{H_{y0}} = -1.41 R_t \left(1 + \frac{P}{P_y}\right)^5 \bar{\lambda}^{1.3} \qquad (5)$$

wherein P/P_y=axial load ratio; δ_{y0} and H_{y0} are the yield displacement and yield load under P/P_y=0.

(2) Hysteretic rules

2-para model takes into account the following observed cyclic behavior through its hysteretic rules: 1) cyclic hardening effect; 2) stiffness degradation; 3) strength degradation. The loading history is divided into two stages in the modeling: the hardening stage and the degrading stage. The hardening stage is the initial loading stage while the displacement stays within $|\delta_m|$, and behavior of the structure is characterized by cyclic hardening effect; the degrading stage begins once the displacement moves out of the range of $|\delta_m|$, and the hysteretic behavior is marked by deterioration of strength.

Stiffness degradation is considered throughout the two stages whenever it comes to determining the slope of the unloading limb; the deterioration of stiffness is related to accumulated hysteretic energy by[1]:

$$\frac{K}{K_1} = 1 - \frac{1}{\alpha} ln\left(\frac{\sum E_i / E_e}{100} + 1\right) \qquad (6)$$

wherein $K_1 = H_y/\delta_y$ is the initial elastic stiffness of the bridge pier and the empirical parameter $\bar{\alpha}$ is determined from extensive FEM analysis results as:

$$\bar{\alpha} = \frac{1}{7.36 R_t} \qquad (7)$$

Note that $E_e = \frac{1}{2} H_y \delta_y$ is used to normalize the accumulated hysteretic energy $\sum E_i$ in Eq.(4).

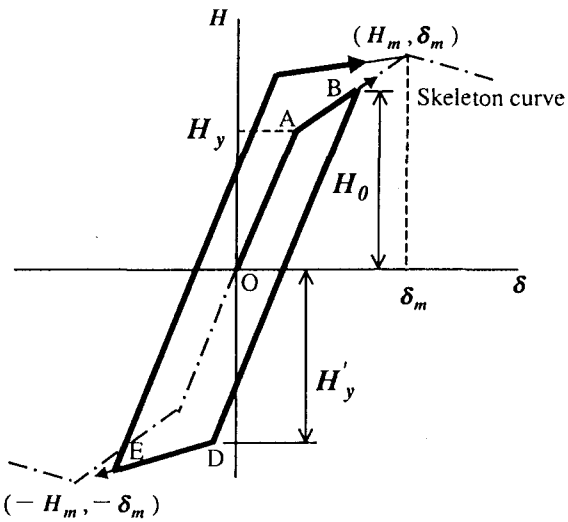

Fig.2 Hysteretic rules of the hardening stage (2-para model)

Fig.2 illustrates the hysteretic rules of the hardening stage. Starting from point O, the initial yield occurs at point A; beyond point A, the loading point follows a plastic hardening limb heading toward peak point of the skeleton curve (H_m, δ_m); suppose before reaching the peak point, there is unloading from point B at a strength level of H_0; cyclic hardening is modeled by stretching the 'elastic' limb beyond the initial yield load H_y when reloading, and the elastic range is now updated to:

$$H'_y = H_y + \gamma(H_0 - H_y) \qquad (8)$$

wherein γ=hardening factor calculated by

$$\gamma = 1.2 - 10 R_t \qquad (0 \le \gamma \le 1) \qquad (9)$$

Beyond the hardened elastic range on the opposite side, the loading point is directed toward peak point of the skeleton curve on the opposite side $(-H_m, -\delta_m)$ (D to E in **Fig.2**); if at unloading from point E, the displacement still falls within hardening stage, the 'elastic' limb will be stretched again, and so on.

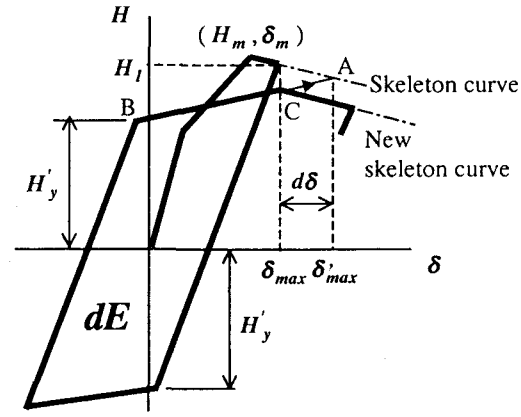

Fig.3 Hysteretic rules of the degrading stage (2-para model)

Now referring to **Fig.3** for an explanation of the hysteretic rules during the degrading stage. Strength degradation is modeled by the following treatments: Firstly, the elastic range starts to shrink, which is expressed by:

$$\begin{aligned} H'_y &= K\delta_y + \gamma(H_1 - H_y) \qquad (if\ H_1 > H_y) \\ H'_y &= K\delta_y \qquad\qquad\qquad\quad (if\ H_1 \le H_y) \end{aligned} \qquad (10)$$

wherein H_1 is the strength at the unloading point in **Fig.3**, and K the current stiffness given by Eq.(4). It is obvious that in Eq.(8) expresses shrinking of elastic range in terms of strength and stiffness deterioration. Secondly, the loading point is directed toward a image point on the descending branch of the skeleton curve after yielding, thus forming a plastic hardening limb (BC in **Fig.3**). The image point (point A in **Fig.3**) is designated by: $\delta'_{max} = \delta_{max} + d\delta$, and $d\delta = \bar{\beta} \cdot dE / H_m$, wherein $\bar{\beta}$ is the strength degradation factor. It is obvious that a larger $\bar{\beta}$ shall result in faster strength degradation. Through careful calibration, parameter $\bar{\beta}$ is given as:

$$\bar{\beta} = \frac{1}{3}(5R_t + 0.25) \qquad (11)$$

Next, motion of the loading point follows a literally

descending branch with the stiffness of K_d if the loading point tends to move beyond the current maximum displacement δ_{max} (motion of the loading point after point C in **Fig.3**). And finally, the latest formed descending branch shall serve as new skeleton curve in determining the image point for further loading cycles on the same side.

3. Damage-based hysteretic model [3)]

The structural characteristics of thin-walled steel bridge piers make them susceptible to damage in the form of local buckling and overall interaction instability. From this point of view, deterioration of strength and stiffness under a seismic event is due to accumulation of damage in the structure. At the center of the damage-based hysteretic model is a comprehensive damage index to quantify the seismic damage throughout the loading history.

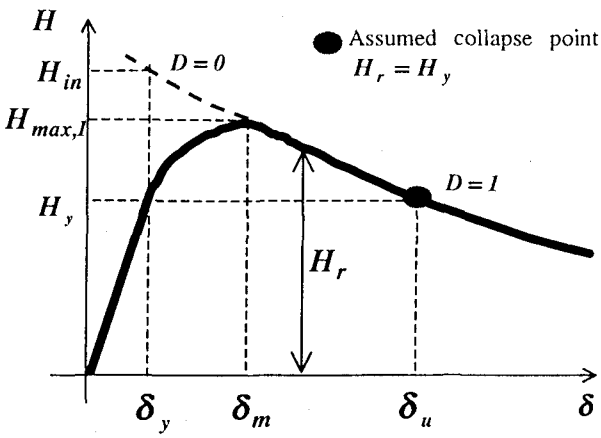

Fig.4 Degradation of strength under monotonic loading (D model)

(1) Damage index formulation

The damage index for thin-walled steel bridge piers is expressed by:

$$D=(1-\beta)\sum_{j=1}^{N_1}\left[\left(\frac{\delta_{max,j}-\delta_y}{\delta_u-\delta_y}\right)^c\right]+\beta\sum_{i=1}^{N}\left[\left(\frac{E_i}{0.5(H_y+H_{max,1})(\delta_u-\delta_y)}\right)^c\right] \quad (12)$$

This damage index formulation consists of two terms: the first term in Eq.(12) considers damage due to large inelastic deformation, and the second term represents damage due to low-cycle fatigue. H_y and δ_y are yield horizontal load and yield horizontal displacement respectively; δ_u is the displacement at collapse under monotonic loading; $\delta_{max,j}$ is maximum absolute displacement for the j-th half-cycle; N_1 is the number of half-cycles producing $\delta_{max,j}$ such that $\delta_{max,j} > \delta_{max,j-1} + \delta_y$ and the initial reference $\delta_{max,0}$ is designated as δ_y; E_i is the hysteretic energy absorbed during the *i-th* half-cycle; Note that an analytical quantity $0.5(H_y+H_{max,1})(\delta_u-\delta_y)$ is used to normalize E_i, wherein $H_{max,1}$ is the maximum strength reached under monotonic loading (see **Fig.4**). β and c are the two free parameters in this damage index formulation. The damage index $D=0$ corresponds to the *initial* undamaged state of the structure; it increases with the onset of inelastic deformation and is supposed to come to unity at collapse. Collapse is defined as the residual strength dropping to yield load H_y (**Fig.4**). With this criterion for collapse, β is fixed at 0.27 and c is related to slenderness ratio by:

$$c=1.69\bar{\lambda}+0.93 \quad (0.20\le\bar{\lambda}\le 0.50) \quad (13)$$

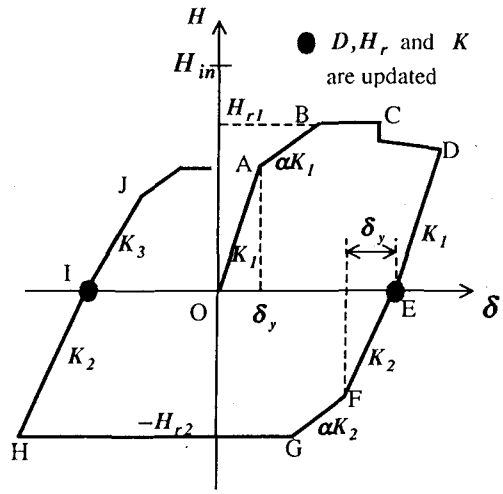

Fig.5 Hysteretic rules (D model)

For pipe-section steel bridge piers, monotonic parameters $H_{max,1}$ and δ_u can be obtained using the following approximate equations:

$$\frac{H_{max,1}}{H_y}=\frac{[0.204(1+P/P_y)]^{4.87}}{(R_t^2\bar{\lambda})^{0.8}}+1.32 \quad (14)$$

$$\frac{\delta_u}{\delta_y}=\frac{0.037}{(1+P/P_y)^{2.5}R_t^{1.89}\bar{\lambda}^{1.14}}+1.15 \quad (15)$$

(2) Damage-based hysteretic model

With the damage quantified by the above damage index, the first step in formulating the restoring force model is relating degradation of strength and stiffness to damage progression:

$$H_r=H_{in}\cdot\left(\frac{H_y}{H_{in}}\right)^D \quad (16)$$

$$K=K_1\cdot\left(\frac{H_y}{H_{in}}\right)^D \quad (17)$$

where K_1 is the initial elastic stiffness; H_{in} is the

imaginary strength at $D=0$. See **Fig.4** for an illustration of strength degradation from H_{in} to H_y at collapse under monotonic loading. Denote the damage index value at $\delta=\delta_m$ $H=H_{max,I}$ in **Fig.4** as D_m, there is $H_{max,I}=H_{in}\cdot(\frac{H_y}{H_{in}})^{D_m}$ according to Eq.(16), thus

$$H_{in}=exp(\frac{ln H_{max,I}-D_m\cdot ln H_y}{1-D_m}) \tag{18}$$

Thus H_{in} depends on calculation of D_m by Eq.(12).

The hysteretic model is of piecewise multi-linear type. Basically the loading branch follows a tri-linear skeleton of an elastic limb, a hardening limb and a perfectly plastic limb. With updating of the damage index and residual strength, there may also be a descending limb in addition to the above three limbs. **Fig.5** illustrates the loading and unloading rules of this model: The loading is initially elastic of stiffness K_I up to point A corresponding to a displacement of δ_y; From point A to point B, the strain hardening stiffness is α times K_I; The point B corresponds to a load of $H_{max}=H_r$, and from point B, a perfectly plastic limb is followed until point C at which the damage index is updated and so is the residual strength; From point C and on, the loading follows a descending limb; Unloading from point D to point E is ruled to have the same stiffness as that of elastic loading OA; At the end of the first half cycle O-A-B-C-D-E, the damage index D, residual strength H_r as well as elastic stiffness K are updated thus reloading in the opposite direction from point E to point F has the updated stiffness of K_2; Point F corresponds to a displacement of δ_y from point E; FG is another strain hardening limb with a stiffness of α times K_2; and a perfectly plastic limb follows point G and so on. It is ruled that D, H_r and K be updated at the end of each half-cycle, and during a loading branch, D and H_r be updated whenever $\delta_{max,j}$ exceeds the recorded maximum so far; thus triggering a descending limb (such as CD in **Fig.5**).

The parameter α defines the ratio of hardening stiffness to elastic stiffness, and can be extracted from the monotonic $H-\delta$ curve under an equal-energy principle[5], that is, in **Fig.6**, area under skeleton O-A-B-C should equal that under actual monotonic curve up to peak point C. It can be inferred that knowing α, δ_m, $H_{max,I}$, as well as the free parameters β and c, the damage index value D_m can be calculated, and in turn H_{in}. Hence D_m as well as H_{in} are taken as secondary quantities while α, δ_m and $H_{max,I}$ are deemed basic parameters of the model. For pipe-section steel bridge piers, the parameter α and δ_m are given as:

$$\alpha=\left(\frac{0.081}{R_t}\right)^{3.93}\bar{\lambda}^{-0.01R_t^{-2}}+6.3R_t-0.1 \tag{19}$$

$$\frac{\delta_m}{\delta_y}=\frac{0.00064}{\left(R_t\sqrt{\bar{\lambda}}\right)^{2.61}}+1.04 \tag{20}$$

Note that δ_m in D model denotes the displacement at the peak of monotonic $H-\delta$ curve, and is different from that of 2-para model.

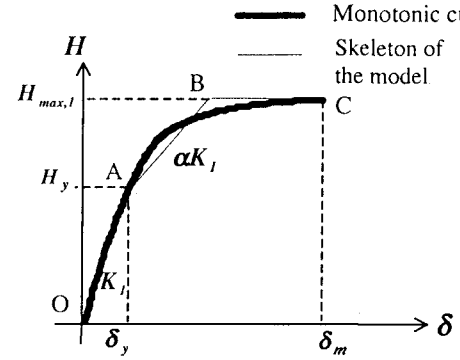

Fig.6 Evaluation of α (D model)

Table 1 Structural parameters of pseudodynamic test specimens

Test specimen	R_t	$\bar{\lambda}$	P/P_y	Mass $(tf\cdot s^2/cm)$	H_y (tf)	δ_y (cm)
TS11-30-16 (JMA)	0.102	0.316	0.155	1.876	545.1	5.94
TS11-30-11 (HKB)	0.119	0.338	0.111	1.508	639.5	7.11
TS11-30-11 (1.5×HKB)	0.117	0.337	0.111	1.518	643.6	7.07
TS08-30-18 (JMA)	0.081	0.318	0.181	2.806	672.8	5.80

Note: Mass, H_y and δ_y have been converted to those of the assumed real bridge piers

4. Simulation of pseudo-dynamic tests

Although 2-para model and D model are formulated based different concepts, both can be classified as evolutionary-degrading restoring force model. D model describes deterioration of strength and stiffness by means of tracing the damage index, while 2-para model uses skeleton curve and progressive hysteretic rules. It should be noted however, concepts of D model enables simulating monotonic behavior while 2-para model applies only to cyclic loading. From this point of view, D model is more comprehensive in formulation. This study, however, will focus on comparing model performance in their major field of application — seismic response analysis.

Employing 2-para model and D model to predict restoring force, time-history analysis is carried out to simulate pseudo-dynamic tests on pipe-section steel bridge piers[6]. The single bridge piers of cantilever type are modeled as SDOF system in the inelastic seismic response analysis. Input earthquake excitations are two accelerograms of Hyogoken-Nanbu earthquake: one was

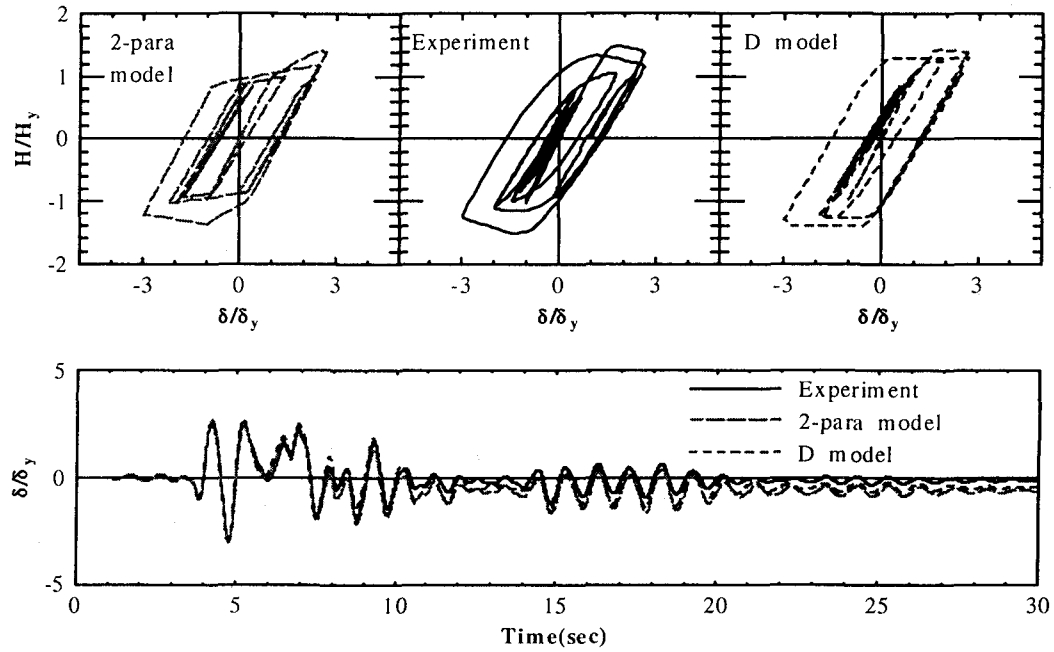

Fig.7 Response of TS11-30-16 to JMA accelerogram

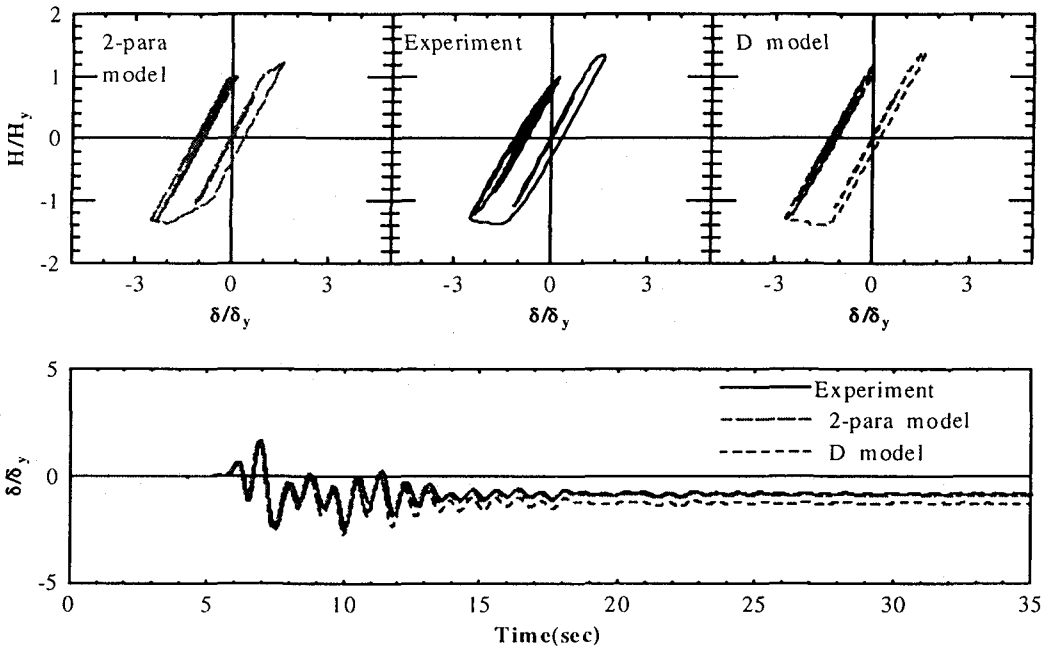

Fig.8 Response of TS11-30-11 to HKB accelerogram

recorded by Japan Meteorological Agency (JMA) (NS component , ground type I) and the other was observed at Higashi Kobe Bridge (HKB) (NS component, ground type III). The linear acceleration method (time interval: $\Delta t = 0.02$ with JMA and $\Delta t = 0.01$ with HKB) is used to solve the equation of motion. Damping ratio is assumed as 0.05 . Structural parameters of the analyzed specimens are listed in **Table 1**. The predicted dynamic responses are compared with test results in **Fig.7-10**. Good agreement in maximum displacement and occasional discrepancies in residual displacement are common to the performance of these two models when it comes to displacement responses. Thus it can be said that major disagreement between the two hysteretic models lies in prediction of residual displacement. It is interesting to note that while 2-para model seems to outperform D model under HKB accelerogram (**Fig.8**), it is D model that provides a closer fit to experimental result under 1.5 ×HKB accelerogram(**Fig.9**). And the test two specimens are almost identical according to **Table 1**. The conspicuous disparity between 2-para model and D model in **Fig.9** may suggest that D model is more stable of the

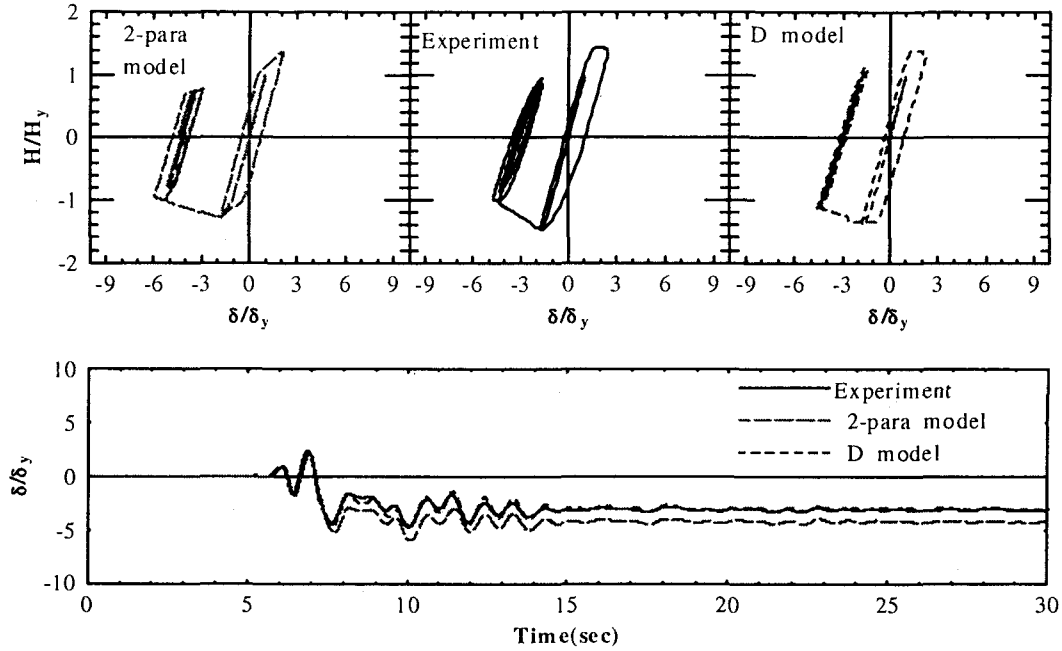

Fig.9 Response of TS11-30-11 to 1.5×HKB accelerogram

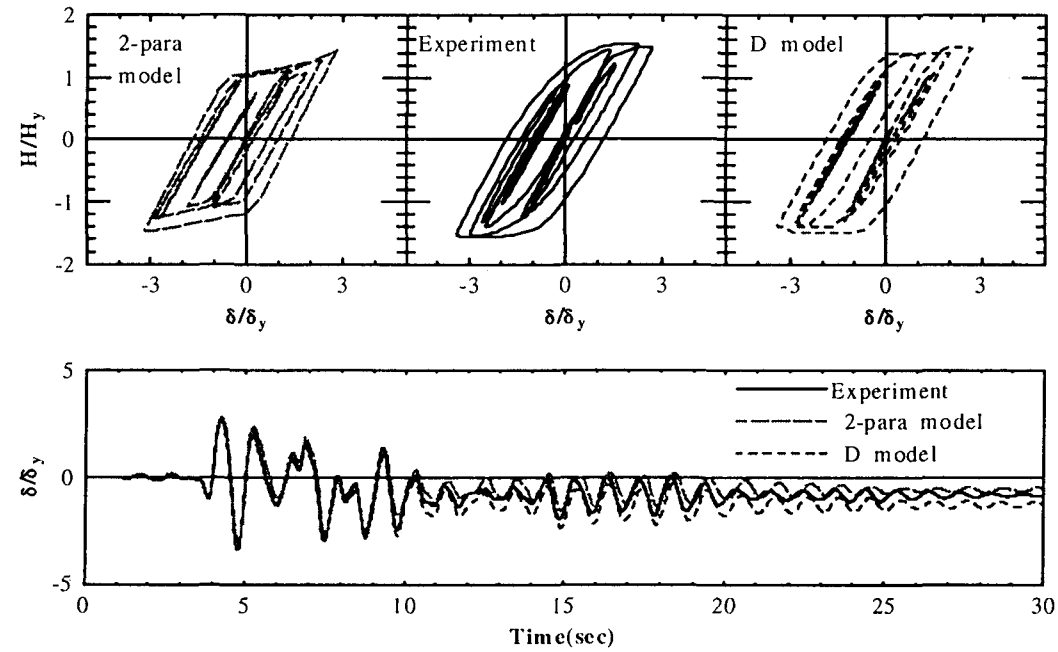

Fig.10 Response of TS08-30-18 to JMA accelerogram

two. Looking at hysteretic loops, it seems that curves from 2-para model are dominated by the hardening limbs, which makes the overall shapes too stiff to be called realistic. It can fairly be said that despite occasional lapse in continuity (when the damage index and strength are updated during a loading session) D model still beats 2-para model in offering more flexible and realistic hysteretic loops.

5. Responses to other accelerograms

To further investigate effect of different hysteretic models on seismic response analysis results, responses of specimen TS08-30-18 (structural parameters listed in **Table 1**) predicted by the two models under other accelerograms are compared in this section. Selected for this purpose are two spectrum-fit accelerograms of Level 2 specified in JRA Specification[7]:

1) ITAJIMA — Level 2, Type I, Ground type II accelerogram;

2) JR-Takatori, N-S component — Level 2, Type II, Ground type II accelerogram modified from the record of

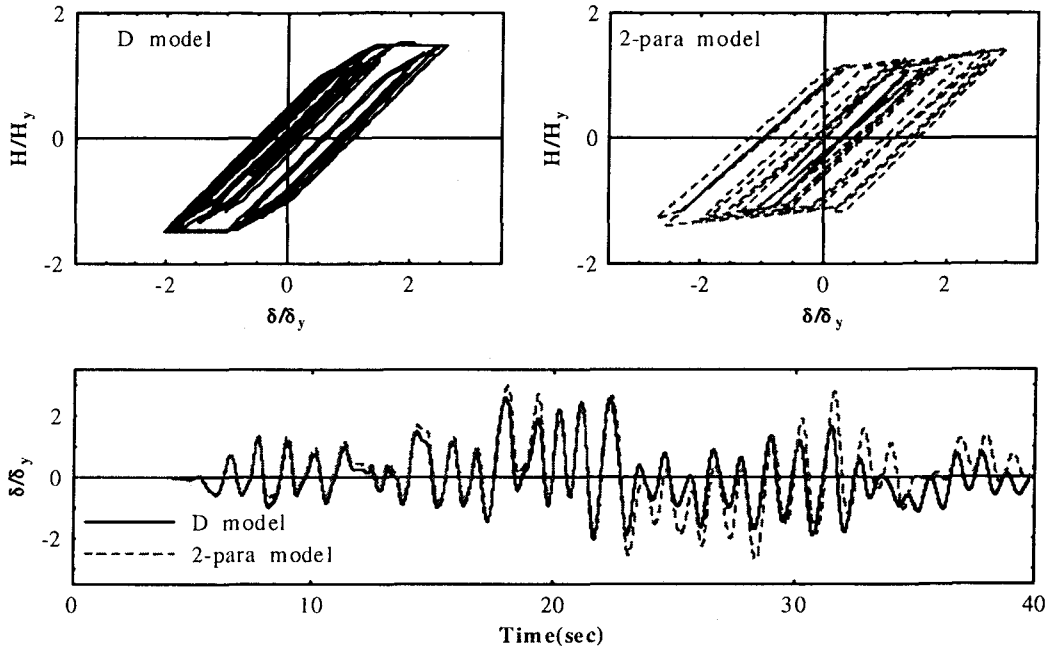

Fig.11 Responses under ITAJIMA accelerogram

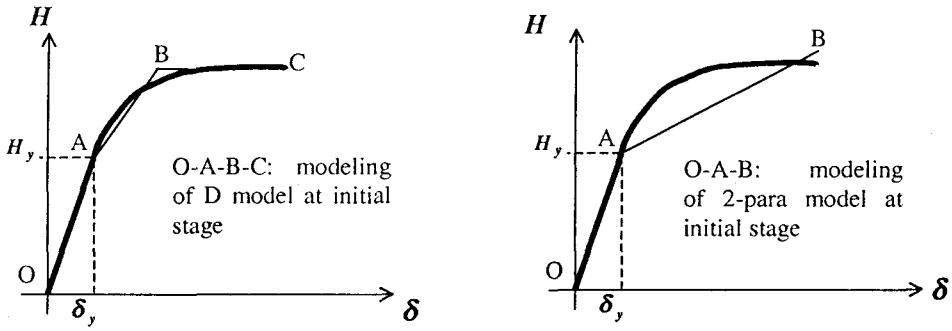

Fig.12 Trilinear modeling and bilinear modeling

Japan Railway Technical Research Institute near JR Takatori station during Hyogoken-Nanbu Earthquake. **Fig.11** shows the predicted response under ITAJIMA accelerogram. The displacement responses are characterized by large number of cycles of small amplitude (just about $\pm 3\delta_y$). D model gives a displacement response varying between $-2.04\delta_y$ and $2.59\delta_y$, while both the maximum and the minimum displacment are amplified under 2-para model ($-2.71\delta_y$ and $2.99\delta_y$ respectively). Due to small displacement amplitude, the hysteretic loops of 2-para model shows the behavior stays within the hardening stage for the most part. Just the opposite of the trend in displacement response, the strength reached under 2-para model is noticeably lower than that predicted by D model. Such a difference can be explained from the very makeup of the two models. Referring to **Fig.12**, it is clear that during the hardening stage defined in the 2-para model, a bilinear curve is used to simulate the hardening behavior of the structure after initial yielding; on the other hand, D model uses a trilinear skeleton to simulate the same behavior. Despite the loading point being directed toward the peak-point of the skeleton curve and considering of cyclic hardening through expanding the nominal elastic range, bilinear modeling still results in a sharp drop in stiffness and more serious discount of strength compared with trilinear modeling. Comparison with experimental results in the last section also indicates such a trend. It is also realized that predicted response under 2-para model is very sensitive to the nominal elastic range.

According to **Fig.13**, JR-Takatori accelerogram inflicts severe one-sided displacement and near-peak residual displacement on the structure. Although the discrepancies between the two models in maximum displacement and in residual displacement are relatively small, it should be noted that the predicted maximum displacement occurs at different time under these two models (at 6.22 second under D model, but at around 15.8 second under 2-para model). Underestimation of strength at the initial stage still marks the hysteretic behavior under 2-para model.

6. Conclusions

By properly adapting model parameters, two hysteretic

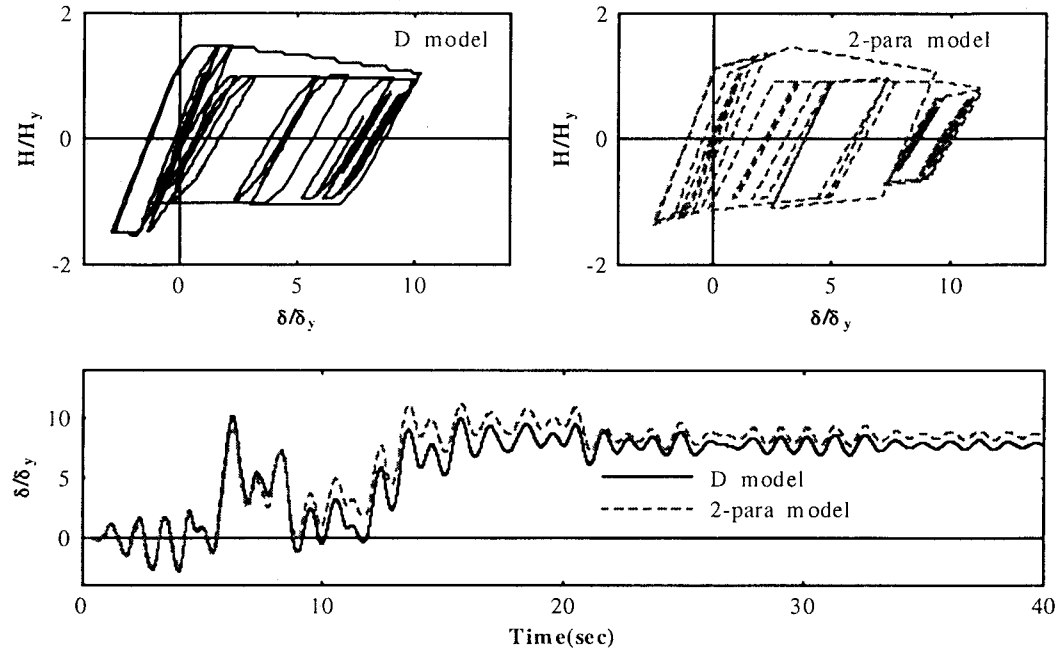

Fig.13 Responses under JR-Takatori accelerogram

models based on tests of box-section steel bridge piers— 2-parameter model and the damage-based hysteretic model are extended to apply to seismic response analysis of pipe-sectoin steel bridge piers. The three model types in the origianl 2-parameter model is integrated into one in the adaptation.

Comparison of predicted seismic responses with limited pseudodynamic test results shows general good agreement between the two models, as well as satisfactory simulation of test results by both models. However, under long-duration accelerograms as well as extremely large displacement, effect of different models on the predicted seimic response can't be neglected. It is the strong recommendation of the authors to use a real trilinear curve to simulate the restoring force, thus allowing for a smoother trasition from linear elastic behavior to degrading behavior in a hysteretic model. Also, since different hysteretic models involve different concepts and assumptions in their formulations, practical application of a certain hysteretic model may require reasonably establishing its application scope in terms of the predicted responses.

Acknowledgements

The authors want to thank the joint research group of Public Works Research Institute, Tokyo Highway Association, Hanshin Highway Association, Nagoya Public Highway Company, Kozai Club Inc. and Japan Bridge Construction Institute Inc. for providing pseudodynamic test data used in this paper.

References

1) M.Suzuki, T. Usami, M. Terada, T. Itoh and K. Saizuka: Hysteretic model and inelastic seismic analysis of box-section steel bridge piers, *Proc. of JSCE*, No.549/I-37, pp.1-14, Oct. 1996 (In Japanese).
2) S. Kumar and T. Usami: An evolutionary-degrading hysteretic model for thin-walled steel structures, *Engineering Structures*, Vol. 18, No.7, pp.504-514, 1996.
3) Qingyun Liu, Akira Kasai and T. Usami: Parameter Identification of Damage-based Hysteretic Model for Pipe-section Steel Bridge Piers, submitted to *Journal of Structural Engineering, JSCE*, 1999.
4) S. B. Gao, T. Usami and H. B. Ge: Ductility Evaluation of Steel Bridge Piers with Pipe Sections, *Journal of Engineering Mechanics, ASCE*, Vol. 124, No.3, pp.260-267, 1998.
5) T. Kindaichi, T. Usami and S. Kumar: A Hysteresis Model Based on Damage Index for Steel Bridge Piers, *Journal of Structural Engineering, JSCE*, Vol. 44A, pp.667-678, March, 1998 (In Japanese).
6) Joint Research Report on Limit State Seismic Design of Highway Bridge Piers (VII), Public Works Research Institute, Tokyo Highway Association, Hanshin Highway Association, Nagoya Public Highway Company, Kozai Club, Inc. and Japan Bridge Construction Institute, Inc., 1997 (in Japanese).
7) Design Specifications of Highway Bridges (Part V. Seismic Design), Japan Road Association, December 1996.